THE JOURNAL OF BIOLOGICAL CHEMISTRY
Vol. 278, No. 2, Issue of January 10, pp. 1101–1107, 2003
© 2003 by The American Society for Biochemistry and Molecular Biology, Inc.
Printed in U.S.A.

Hypertonicity Is Involved in Redirecting the Aquaporin-2 Water Channel into the Basolateral, Instead of the Apical, Plasma Membrane of Renal Epithelial Cells*

Received for publication, July 22, 2002, and in revised form, September 13, 2002
Published, JBC Papers in Press, October 8, 2002, DOI 10.1074/jbc.M207339200

Bas W. M. van Balkom‡, Marcel van Raak‡, Sylvie Breton§¶, Nuria Pastor-Soler§‖, Richard Bouley§‖, Peter van der Sluijs, Dennis Brown§‡‡, and Peter M. T. Deen‡§§**

*From the ‡Department of Cell Physiology, Nijmegen Center for Molecular Life Sciences, UMC St. Radboud, Nijmegen, 6500 HB, The Netherlands, the §Program in Membrane Biology and Renal Unit, Department of Medicine, Massachusetts General Hospital and Harvard Medical School, Charlestown, Massachusetts 02129, and the **Department of Cell Biology, University of Utrecht, 3584 CX Utrecht, The Netherlands*

In renal collecting ducts, vasopressin increases the expression of and redistributes aquaporin-2 (AQP2) water channels from intracellular vesicles to the apical membrane, leading to urine concentration. However, basolateral membrane expression of AQP2, in addition to AQP3 and AQP4, is often detected in inner medullary principal cells *in vivo*. Here, potential mechanisms that regulate apical *versus* basolateral targeting of AQP2 were examined. The lack of AQP2–4 association into heterotetramers and the complete apical expression of AQP2 when highly expressed in Madin-Darby canine kidney cells indicated that neither heterotetramerization of AQP2 with AQP3 and/or AQP4, nor high expression levels of AQP2 explained the basolateral AQP2 localization. However, long term hypertonicity, a feature of the inner medullary interstitium, resulted in an insertion of AQP2 into the basolateral membrane of Madin-Darby canine kidney cells after acute forskolin stimulation. Similarly, a marked insertion of AQP2 into the basolateral membrane of principal cells was observed in the distal inner medulla from normal rats and Brattleboro rats after acute vasopressin treatment of tissue slices that had been chronically treated with vasopressin to increase interstitial osmolality in the medulla, but not in tissues from vasopressin-deficient Brattleboro rats. These data reveal for the first time that chronic hypertonicity can program cells *in vitro* and *in vivo* to change the insertion of a protein into the basolateral membrane instead of the apical membrane.

The renal collecting duct is involved in urine concentration via a process that is regulated by the antidiuretic hormone arginine vasopressin (AVP).[1] After binding to its receptor on target cells in the kidney collecting duct, AVP initiates an intracellular signaling cascade that increases cytosolic cAMP and calcium levels (1–3). Upon activation of protein kinase A, aquaporin-2 (AQP2) is phosphorylated and is rapidly redistributed from intracellular vesicles to the apical membrane of collecting duct principal cells. Driven by an osmotic gradient, water then moves into the cell apically via AQP2, and exits across the basolateral membrane via AQP3 and/or AQP4 (4, 5). In addition to this short term effect, increased circulating AVP levels also lead to an increased expression of AQP2 protein, which is mediated via a cAMP responsive element in the AQP2 gene promoter (6–8). Additionally, the expression of AQP3 is increased, but the level of AQP4 remains unchanged (9, 10).

Although the majority of AQP2 is located in the apical plasma membrane under "steady-state" conditions in normally hydrated animals, immunocytochemical studies have shown that AQP2 antigenicity can also be detected in the basolateral plasma membrane of collecting duct principal cells in these rats. This basolateral staining pattern becomes more prominent with increased AVP levels or water deprivation in rats, and is especially prominent in the principal cells of the inner medulla (11).

The factors and mechanisms that determine the partitioning of AQP2 between the apical and basolateral membrane of principal cells in the kidney are unknown, and the goal of the present study was to investigate this process further. Three hypotheses that might explain basolateral AQP2 targeting were tested using renal tissue, as well as oocytes and cultured renal epithelial cells heterologously expressing AQP2, AQP3, and/or AQP4. We considered (*a*) that heterotetramer formation among differentially targeted aquaporins might be involved, (*b*) that higher levels of AQP2 expression both *in vivo* and *in vitro* might cause AQP2 to traffic to the membrane in both apical and basolateral pathways, and (*c*) that a hypertonic environment such as that found in the renal medullary interstitium could play a role. Our data indicate that long term exposure of cells to hypertonicity primes epithelial cells to insert AQP2 into the basolateral membrane upon acute stimulation with AVP and/or forskolin.

EXPERIMENTAL PROCEDURES

Plasmids—To stably express AQP2 in MDCK cells in high amounts, the pBS-AQP2 (12) construct was digested with *Xba*I, blunted, and cut with *Hin*dIII. Subsequently, the full-length human AQP2 cDNA was isolated and ligated into the blunted *Bgl*II site and *Hin*dIII site of the

* This work was supported in part by Dutch Organization of Scientific Research Grant NWO-MW 902-18-092 (to P. M. T. D. and P. v. d. S.) and European Union Grant QLRT-2000-00778 (to P. M. T. D.). The costs of publication of this article were defrayed in part by the payment of page charges. This article must therefore be hereby marked "*advertisement*" in accordance with 18 U.S.C. Section 1734 solely to indicate this fact.

¶ Supported by National Research Service Award, National Institutes of Health Grant HD08684.

‖ Supported by a grant from the National Kidney Foundation and National Institutes of Health Grant DK38452.

‡‡ Supported by National Institutes of Health Grant DK38452.

§§ To whom correspondence should be addressed: 160, Dept. of Cell Physiology, UMC St. Radboud Nijmegen, P. O. Box 9101, 6500 HB Nijmegen, The Netherlands. Tel.: 31-24-3617347; Fax: 31-24-3616413; E-mail: p.deen@ncmls.kun.nl.

[1] The abbreviations used are: AVP, arginine vasopressin; AQP2, aquaporin-2; MDCK, Madin-Darby canine kidney; dDAVP, 1-desamino-8-D-arginine vasopressin ; IOD, integrated optical density.

Downloaded from http://www.jbc.org/ at Universiteitsbibliotheek Utrecht on June 14, 2018

eucaryotic expression vector pCB6 (13), thereby generating pCB6-AQP2. To generate the oocyte expression construct pT7Ts-AQP4, a pBluescript vector containing the entire cDNA of human AQP4a (pBS-AQP4a (14)) was digested with *Eco*RV and *Xba*I, full-length AQP4a cDNA was isolated and cloned into the *Eco*RV and *Spe*I sites of pT7Ts. The pSPORT-AQP3 construct, encoding full-length rat AQP3 (15), was kindly donated by M. Echevarria, Sevilla, Spain.

AQP Expression in Oocytes—*Xenopus laevis* oocytes were isolated and cultured as described (16). To generate AQP2, AQP3, and AQP4 cRNAs, pT7Ts-AQP2 (17) was linearized with *Sal*I, whereas pSPORT-AQP3 and pT7Ts-AQP4 were linearized with *Xba*I. Synthesis of G-capped cRNA transcripts and determination of their integrity and concentration were done as described (17). Two days after injection, oocytes were subjected to assays described below.

Culturing and Transfection of MDCK Cells—All cells used in this study were derived from MDCK type I cells (18) and were grown in Dulbecco's modified Eagle's medium supplemented with 5% (v/v) fetal calf serum at 37 °C in 5% CO_2. Transfected cells used were those stably expressing human AQP2 (Wt10 cells (19)). To obtain MDCK cells expressing high levels of AQP2, MDCK cells stably transfected with the pCB6-AQP2 construct were generated as described (20).

To test the effect of hypertonicity on the steady state localization of AQP2, cells were seeded on 1.13-cm^2 filters at 3.0×10^5 cells/cm^2 and grown in medium for 8 h. Subsequently, the osmolarity of the medium was increased from 297 to 672 mosmol/kg of H_2O in three steps of 125 mosmol/kg of H_2O at $t = 8$, 24, and 32 h using NaCl, sucrose, raffinose, or mannitol as osmolytes. The MDCK cells were analyzed at 3 days after seeding, which meant that the cells were exposed to hypertonicity for about 64 h (starting 8 h after seeding) and to a full hypertonicity (672 mosmol/kg) for 40 h. Control cells were seeded at 1.5×10^5 cells per cm^2. Three days after seeding, the cells were directly prepared for confocal laser scanning microscopy analysis or first incubated for 45 min in hypertonic medium containing 1×10^{-5} M forskolin to induce translocation of AQP2 to the plasma membrane (19).

Isolation of Membranes—Total membranes of oocytes were isolated as described previously (16). For membranes of renal cells, kidneys were removed from control or 24-h water-deprived rats and homogenized in 5 ml of HbA per 350 mg of wet tissue. After removing nuclei and unbroken cells by centrifugation at $1000 \times g$ at 4 °C for 10 min, each supernatant was centrifuged at $100{,}000 \times g$ for 1 h to pellet the membranes.

Subsequently, oocyte (20 μl/oocyte) and kidney (5 ml/sample) membranes were incubated for 30 min at 37 °C in solubilization buffer (4% Na-desoxycholate, 20 mM Tris (pH 8.0), 5 mM EDTA, 10% glycerol, 1 mM phenylmethylsulfonyl fluoride, 5 μg/ml leupeptin and pepstatin) to dissolve the membranes. Next, undissolved membranes were removed with a centrifugation step at $100{,}000 \times g$ at 4 °C for 1 h.

Antibodies—For analysis of AQP2, rabbit (17) and guinea pig (21) antibodies, raised against a synthetic peptide corresponding to the last 15 amino acids of rat AQP2 were used. AQP3 antibodies were raised against a peptide based on the predicted 15 COOH-terminal amino acids of rat AQP3, which was conjugated to keyhole limpet hemocyanin (17). By passing whole serum over a bovine serum albumin-AQP3-coupled Affi-Gel 15 column, affinity purified antibodies were isolated (Amersham Biosciences, Uppsala, Sweden). Antibodies were eluted with 0.1 M glycine (pH 2.8) and directly neutralized.

To generate AQP4 antibodies, a fragment of 389 nucleotides encoding the entire C-terminal tail of AQP4a was isolated from pBS-AQP4a, by digestion with *Eco*RI, and cloned into the *Eco*RI site of the pGEX1 vector (Amersham Biosciences). After transformation of DH5α bacteria with this construct and induction of protein expression with isopropyl-1-thio-β-D-galactopyranoside, the soluble glutathione *S*-transferase-AQP4 fusion protein was isolated using glutathione-Sepharose 4B (Amersham Biosciences). Antibodies raised in rabbit and guinea pig were affinity purified as described above.

Immunoprecipitations and Sucrose Gradient Analysis—Immunoprecipitations were performed as previously described (16). Samples (300 μl) of solubilized renal and oocyte membranes were loaded onto a 3.2-ml 5–17.5% linear sucrose gradient (in 20 mM Tris (pH 8.0), 5 mM EDTA, 0.1% Triton X-100, 1 mM phenylmethylsulfonyl fluoride, 5 μg/ml leupeptin and pepstatin). Gradients were centrifuged at $100{,}000 \times g$ in a Beckman SW-60 rotor for 16 h at 8 °C. After centrifugation, 200-μl fractions, annotated A–Q, were taken from the top and 15-μl samples were analyzed by immunoblotting. As size markers, bovine serum albumin (68 kDa), phosphorylase *b* (97 kDa), yeast alcohol dehydrogenase (150 kDa), and β-amylase (200 kDa) were centrifuged in a parallel tube. To determine the peak fractions of marker proteins, fractions were analyzed by SDS-PAGE, after which the proteins were visualized using Coomassie Brilliant Blue staining.

Immunoblotting—To prepare Wt10 cell lysates, cells from a 1.13-cm^2 filter were incubated in 170 μl of Laemmli buffer for 30 min, after which the DNA was sheared by pulling the sample through a 30-gauge needle 3 times. When indicated, *N*-linked sugar groups were removed with peptide *N*-glycosidase F according to the manufacturer (New England Biolabs, Beverly, MA). Samples were denatured for 30 min at 37 °C in Laemmli buffer and subjected to 13% SDS-PAGE electrophoresis. Proteins were transferred to polyvinylidene difluoride membranes (Millipore Corp., Bedford, MA) as described (17). For immunoblot analysis, AQP3 antibodies were biotinylated with Sulfo-NHS biotin (Pierce) according the manufacturer. Membranes were incubated with 1:4000 diluted guinea pig AQP2 antibodies in TBST (20 mM Tris, 140 mM NaCl, 0.2% Tween 20 (pH 7.6)), 1:3000 diluted rabbit AQP2 antibodies, 1:1000 biotinylated rabbit AQP3 antibodies or guinea pig AQP4 antibodies, or 1:1000 mouse monoclonal AQP1 antibodies (22), which were all diluted in TBST with 1% nonfat dried milk. As secondary antibodies, goat anti-rabbit (1:5000 in TBST; Sigma), sheep anti-mouse (1:2000 in TBST; Sigma), goat anti-guinea pig (1:10,000 in TBST; Sigma), or streptavidin (1:8000 in TBST with 1% nonfat dried milk; Jackson ImmunoResearch, West Grove, PA), all coupled to horseradish peroxidase, were used. Proteins were visualized using enhanced chemiluminescence (Pierce).

Confocal Laser Scanning Microscopy on Cell Cultures—Preparation of MDCK cells for CLSM analysis was done as described (20). The filters were incubated overnight with 1:100 diluted affinity purified rabbit anti-AQP2, followed by an incubation with 1:100 diluted Alexa-594-coupled goat anti-rabbit antibodies (Molecular Probes, Eugene, OR). When co-stained for AQP3, 1:100 dilutions of affinity purified rabbit anti-AQP3 and guinea pig anti-AQP2 antibodies were used, followed by 1:100 dilutions of affinity purified goat anti-rabbit or guinea pig IgGs, coupled to Alexa-488 or Alexa-594 (Molecular Probes, Leiden, The Netherlands), respectively. Using Adobe Photoshop, all signals were maximally expanded over the intensity range. All figures shown are representative images of at least three independent experiments.

Whole Animal Studies—Animal experiments were approved by the Institutional Committee on Research Animal Care of the Massachusetts General Hospital, in accordance with the NIH guide for the Care and Use of Laboratory Animals. Male adult Sprague-Dawley and homozygous, vasopressin-deficient Brattleboro rats were purchased from Harlan Sprague-Dawley (Indianapolis, IN).

Chronic Vasopressin Treatment of Brattleboro Rats—Adult male Brattleboro homozygous rats weighing 300–360 g were used to study the effects of chronic AVP pretreatment on the polarity of AQP2 membrane insertion after acute AVP treatment in the tissue slice preparation. The Brattleboro rats were divided into two groups (3 animals/group). One group of animals was not treated (control) and the other group received the vasopressin analogue 1-desamino-8-D-arginine vasopressin (dDAVP) at a rate of 5 μl/h via osmotic minipumps as described (23). This dose has been shown to produce comparable plasma vasopressin levels to those achieved in normal rats during water restriction (24). All Brattleboro rats had free access to food and water for the duration of the studies. A 5500 Wescor vapor pressure osmometer (Wescor, Logan, UT) was used to measure the urine osmolarity. Urine samples were collected by "clean catch" before and after the implantation of the minipumps, and at various times during the 11-day treatment period.

Acute Effects of Vasopressin in Control Rat Kidney Slices—Adult Brattleboro rats, pretreated for 11 days (see above), and male Sprague-Dawley rats were anesthetized with an injection of sodium pentobarbital (65 mg/kg; intraperitoneally). Both kidneys were removed from the rats, cut into ~2–3 mm thick slices using a razor blade, and quickly placed in Hanks' balanced salt solution (pH 7.4) at 37 °C equilibrated with 5% CO_2, 95% O_2. Slices of 0.5 mm were then cut as described (25). The thin slices were first incubated at 37 °C for 15 min in equilibrated Hanks' balanced salt solution only (vial A) to wash out endogenous AVP and cause internalization of cell-surface AQP2. These slices were then simultaneously transferred to fresh vials containing either arginine AVP (10 nM) plus forskolin (10 μM) (Sigma) in Hanks' balanced salt solution (vial B) or to vials containing Hanks' balanced salt solution alone (vial C) for 15 min at 37 °C. Next, all slices were fixed by immersion in periodate-lysine containing 4% paraformaldehyde as described (25). Slices were then rinsed several times in phosphate-buffered saline and stored in phosphate-buffered saline containing 0.02% NaN_3 at 4 °C. To determine the localization of AQP2 prior to treatment with AVP plus forskolin, some slices from vial A were fixed immediately. Additionally, some kidney slices from Brattleboro rats were fixed in paraformaldehyde immediately after preparation (*i.e.* before (dD)AVP washout).

Downloaded from http://www.jbc.org/ at Universiteitsbibliotheek Utrecht on June 14, 2018

Immunocytochemistry on Tissue Slices—Kidney cryosections (4 μm thick) were prepared as described (26). After rehydration in phosphate-buffered saline for 15 min, sections were treated with 1% SDS for antigen retrieval (27). Blocking and immunostaining of the sections was done as described (26), except that affinity purified antiserum raised against the second extracellular loop of AQP2 (28) and goat anti-rabbit IgG conjugated to indocarbocyanine (CY3) (2 μg/ml; Jackson ImmunoResearch) were used as primary and secondary antibodies, respectively. Sections were mounted in Vectashield diluted 1:1 in 1.5 M Tris-HCl (pH 8.9). Sections were examined using a Bio-Rad Radiance 2000 confocal laser scanning microscope (Bio-Rad Microscience Ltd., Hemel Hempstead, United Kingdom) or a Nikon 800 epifluorescence microscope coupled to a Hamamatsu Orca CCD camera and IP Lab Spectrum software (Scanalytics, Vienna, VA).

Image Quantification Analysis—To create an objective index for basolateral *versus* apical expression of AQP2, the integrated optical density (IOD) of equal basolateral or apical membrane segments within a fixed square area was determined using Image-Pro Plus analysis software (Media Cybernetics, Silver Spring, MD). Background IOD values, determined within the nucleus area of the particular cell, were subtracted from the obtained basolateral and apical IOD values. The $_{B/A}$sorting index is defined as the IOD of the basolateral membrane segment divided by the IOD of the apical membrane segment. Of 8 or 15 independent cells (indicated) of representative images, and 3 segments of the basolateral and apical membrane per cell, the mean $_{B/A}$sorting index ± S.E. was determined. The significance of a change in sorting index between two experimental settings was determined with an independent two population *t* test.

RESULTS

AQP2, AQP3, and AQP4 Do Not Form Heterotetramers

Some membrane proteins that are mostly expressed as homomultimeric proteins can also form heteromultimeric complexes consisting of related, but distinct, subunits (29, 30). The function, trafficking, and regulation of such heteromeric complexes, such as the heterodimeric $GABA_{B1-2}$ receptor (31), α-amino-3-hydroxy-5-methyl-4-isoxazole propionate receptor (32), and the opioid receptor (33) are different from that of homomeric complexes. Within the AQP family of proteins, altered trafficking of wt-AQP2 has been found upon formation of heterotetramers with the AQP2 mutants AQP2-E258K or AQP2-delG, and this provided the explanation for the occurrence of a dominant form of NDI (16, 34). Whereas all AQPs tested up to now (AQP0-AQP2 and AQP4) are expressed as homotetramers (16, 35–37), the possibility existed that some AQP2 might be targeted to the basolateral membrane because of the formation of heterotetramers with AQP3 and/or AQP4, which are both basolateral membrane proteins.

Aquaporin-3 Is Expressed as Tetramers—To be able to address this hypothesis, it is essential that AQP2, AQP3, and AQP4 are all expressed as tetramers and that the tetramers are not disrupted by the membrane isolation and extraction procedure. Whereas it has been shown that AQP2 and AQP4 form homotetramers (16, 37), this has not been reported for AQP3. To allow these analyses, antibodies were raised against AQP3 and AQP4, affinity purified, and tested for their AQP specificity. Immunoblotting of total membranes from AQP2-, AQP3-, or AQP4-expressing oocytes revealed that each of these antibodies specifically recognized the AQP against which it was raised (not shown). Next, membranes of oocytes expressing AQP2, AQP3, or AQP4 were isolated, solubilized, and sedimented through a sucrose gradient. Immunoblotting of fractions taken from these gradients revealed that AQP3 peaked in fraction J (Fig. 1) between the 97- and 150-kDa marker proteins that were run in parallel. Because an AQP3 monomer has a calculated molecular mass of 31.4 kDa, the observed sedimentation is consistent with the presence of an AQP3 homotetramer. AQP4 bands of 32 and 34 kDa were obtained, which are, as shown before (38), derived from the use of alternative translational starting methionines (M1 and M23), both of which are contained in the AQP4 cDNA construct used here. AQP2 and AQP4, with monomeric molecular masses of 29 and 32/34 kDa, respectively, also peaked in fraction J, which also supports the presence of homotetramers. These data revealed that, besides AQP2 and AQP4, AQP3 is also expressed as homotetramers and that the tetrameric structure remains intact upon solubilization of membranes with desoxycholate.

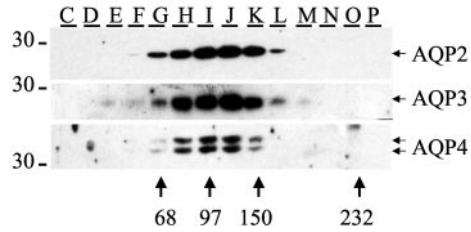

FIG. 1. **AQP3 is expressed as a homotetramer.** Two days after injection, total membranes of oocytes expressing AQP2, AQP3, or AQP4 were isolated, solubilized in desoxycholate, and subjected to sucrose gradient centrifugation. Fractions of 200 μl were taken, of which fractions C to P (indicated) were immunoblotted for AQP2, AQP3, or AQP4. AQP3 fractions were treated with peptide *N*-glycosidase-F before loading. To estimate the mass of the AQP complexes, sedimentation marker proteins, bovine serum albumin (68 kDa), phosphorylase *b* (97 kDa), yeast alcohol dehydrogenase (150 kDa), and β-amylase (200 kDa) were sedimented in a parallel tube. Their peak fractions are indicated at the *bottom*. The mass of a marker protein (in kDa) is given on the *left*. All aquaporins sedimented between the 97- and 150-kDa markers, indicating a tetrameric assembly, which was maintained throughout the extraction and centrifugation procedure.

Do Aquaporins Form Heterotetramers?—To investigate whether AQP2, AQP3, and AQP4 form heterotetramers *in vivo*, rats either received water *ad libitum*, or were water deprived for 24 h to increase the expression of AQP2 and AQP3, and to maximize basolateral expression of AQP2 (11). Total kidney membranes were isolated, solubilized, and subjected to AQP-specific immunoprecipitation. As shown in Fig. 2*A*, none of the other AQPs co-precipitated with the immunoprecipitated AQP. However, AQP2, AQP3 and, to a lesser extent, AQP4 were readily detectable in the lanes containing total kidney membranes. These results indicate that none of the AQPs form heterotetramers. Note that only the 32-kDa isoform of AQP4 was detected in these experiments, which is more abundant in the kidney (37).

In collecting duct cells of water-deprived rats, the majority of AQP2 is still located in the apical membrane and a relative small number of AQP2/AQP3 or AQP2/AQP4 heterotetramers might have been overlooked. Therefore, to examine this further, the three aquaporins were co-expressed in oocytes, where they are all located in the plasma membrane (15, 17, 38). Immunoblotting of the immunoprecipitates for the different AQPs clearly demonstrated that the AQPs did not co-precipitate, even though each AQP was expressed at a high level in this system (Fig. 2*B, TM*). These data show that AQP2, AQP3, and AQP4 are not able to form heteroligomers and, therefore, strongly suggest that the basolateral localization of AQP2 is not a result of heterotetramerization of AQP2 with AQP3 or AQP4. The ~32-kDa AQP3 band on blots disappeared upon digestion with peptide *N*-glycosidase F, indicating that this band corresponded to glycosylated AQP3 (not shown).

Increased Expression of AQP2 Does Not Lead to Its Basolateral Localization

Although most AQP2 is still found in the apical membrane, basolateral expression of AQP2 is especially prominent in antidiuresis. Because in this condition AQP2 expression is increased (6, 11), we speculated that this might lead to expression in the basolateral membrane because of saturation of the apical sorting pathway, and "overflow" of AQP2 into the basolateral pathway. This hypothesis was tested using MDCK cells

Downloaded from http://www.jbc.org/ at Universiteitsbibliotheek Utrecht on June 14, 2018

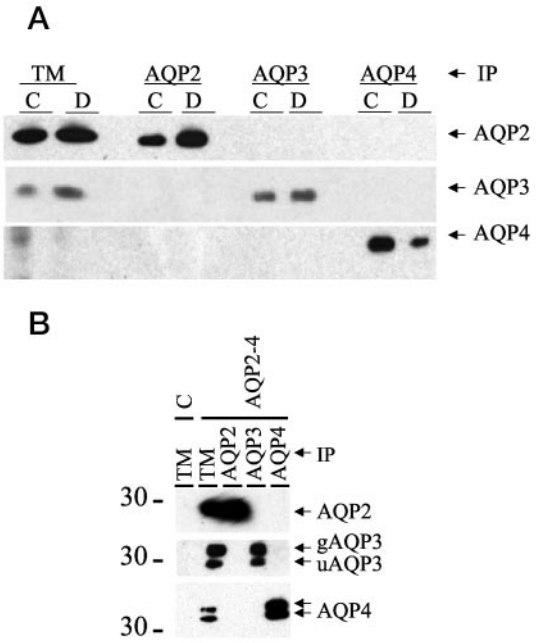

FIG. 2. **AQP2, AQP3, and AQP4 do not form heterotetramers *in vivo* and *in vitro*.** *A*, *in vivo*. Membranes of renal medulla from control (*C*) or water-deprived (*D*) rats were isolated, solubilized in desoxycholate, and subjected to immunoprecipitation (*IP*) with AQP2-, AQP3-, or AQP4-specific antibodies. The proteins of the precipitates were separated by SDS-PAGE and immunoblotted for AQP2 (*upper panel*), AQP3 (*middle panel*), or AQP4 (*lower panel*). Proteins from total membranes (*TM*) of renal medullas were taken as controls. *B*, *in vitro*. Oocytes were injected with a mixture of cRNAs encoding AQP2, AQP3, and AQP4. Two days after injection, membranes were isolated, solubilized in desoxycholate, and analyzed as under *A*. Proteins from total membranes of noninjected (*C*) or AQP2–4 expressing oocytes were taken as negative and positive controls, respectively. In addition to AQP2 and AQP4, unglycosylated (*uAQP3*) and glycosylated AQP3 (*gAQP3*) are indicated. The mass of a marker protein (in kDa) is given on the *left*. These data indicate that AQP2, AQP3, and AQP4 do not form heterotetramers in renal medullas and in oocytes expressing all three aquaporins, because only the aquaporin that was specifically immunoprecipitated is detectable in the respective lanes.

that express AQP2 at moderate levels, driven by an SV40 promoter (Wt10 cells), or at high levels driven by a strong cytomegalovirus promoter. As previously reported (19), confocal microscopy showed that cells with a moderate expression level inserted AQP2 into the apical membrane upon stimulation with forskolin (Fig. 3*A*). Similarly, cells with high AQP2 expression also inserted AQP2 apically (Fig. 3*B*). Semiquantification of the AQP2 expression in the basolateral *versus* apical membrane in Wt10 cells resulted in a $_{B/A}$sorting index of 0.07 ± 0.00 ($n = 8$), which indicated that at these detection levels nearly 20 times more AQP2 was present in the apical than basolateral membrane. In the cells in which AQP2 expression was derived from the cytomegalovirus promoter, no basolateral membrane AQP2 expression was detected, whereas the AQP2 expression in the apical membrane was saturated. These results indicate that basolateral localization of AQP2 is probably not because of saturation of the apical sorting pathway, at least in this culture system.

Hypertonicity Results in the Basolateral Localization of AQP2 in MDCK Cells

Because in antidiuresis, the tonicity of the inner medullary collecting duct is increased (39), we tested whether basolateral targeting of AQP2 could be induced by hypertonicity. The osmolarity of the medium of Wt10 cells was gradually increased with NaCl from 297 to 672 mosmol/kg of H_2O over a 3-day period. Cells were either untreated or exposed to forskolin,

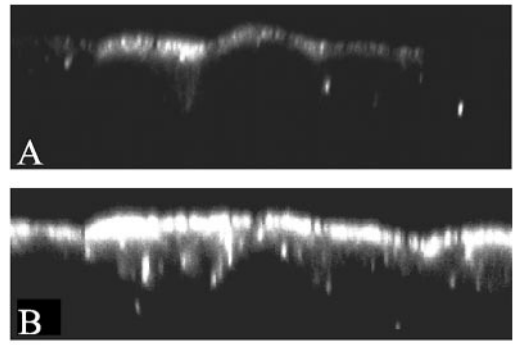

FIG. 3. **Intracellular localization of AQP2 with overexpression.** X-Z images of AQP2 localization in MDCK cells with moderate expression of AQP2 (Wt10 cells; *panel A*) and pooled colonies of MDCK expressing high levels of AQP2 (derived from pCB6-AQP2 construct; *panel B*). The cells were grown to confluence in normal medium, treated with forskolin, fixed, and subjected to AQP2 immunocytochemistry and confocal laser scanning microscopy. For both figures, identical CLSM settings were used.

fixed, and examined by immunocytochemistry. Confocal analysis revealed that without forskolin, AQP2 was mainly localized in vesicles (Fig. 4, *C1* and *H1*). With forskolin stimulation, however, hypertonicity indeed resulted in a pronounced basolateral localization of AQP2 (Fig. 4, *H2*), which was underscored by its co-localization with AQP3 (Fig. 4, *H*, *AQP3*). As reported (40), AQP3 appeared to be induced in its expression in MDCK cells by hypertonicity (not shown) and has shown to be localized in the basolateral membrane (40, 41). The $_{B/A}$sorting index was 1.02 ± 0.04 ($n = 8$; Fig. 4, *H2*), which indicated that with hypertonicity the basolateral *versus* apical expression of AQP2 was about 14-fold increased compared with Wt10 cells grown under isotonic conditions (0.07 ± 0.00; $n = 8$; $p < 0.001$; Fig. 4, *C2*). To further test whether this was osmolyte-dependent, Wt10 cells were treated as above, using different sugars as osmolytes. Confocal analysis of these cells and subsequent determination of $_{B/A}$sorting indexes revealed that compared with cells grown under isotonic conditions, basolateral *versus* apical expression of AQP2 was 15–17-fold increased for mannitol (index of 1.20 ± 0.14; $n = 8$), sucrose (1.08 ± 0.04; $n = 8$), or raffinose (1.22 ± 0.05; $n = 8$) upon forskolin treatment ($p < 0.001$; shown for mannitol in Fig. 4, *H3*).

Basolateral Localization of AQP2 in Kidney Principal Cells in Situ

Previous studies have demonstrated that AQP2 can be detected on the basolateral plasma membrane of collecting duct principal cells *in situ*, and that this basolateral location is (*a*) more prominent in the inner medulla and (*b*) increased after vasopressin treatment or dehydration. To examine this further, experiments on normal rats and vasopressin-deficient Brattleboro rats were performed.

Effect of Acute Vasopressin Treatment on AQP2 Distribution in Normal Rat Kidney Slices—Kidney slices were prepared from normally hydrated Sprague-Dawley rats, and were incubated *in vitro* with and without vasopressin/forskolin. Confocal analysis revealed a heterogeneous pattern of AQP2 distribution in collecting duct principal cells that was different in various regions of the kidney. After removal from the animal and incubation *in vitro* in buffer alone to wash out endogenous vasopressin, plasma membrane staining was considerably reduced (Figs. 5, *A* and *C*) compared with tissues that had been exposed to vasopressin/forskolin (Fig. 5, *B* and *D*). However, a remarkable difference in the polarity of AQP2 insertion was seen between the proximal third and the distal portion of the inner medullary collecting duct. As seen in Fig. 5*B*, a strong

Downloaded from http://www.jbc.org/ at Universiteitsbibliotheek Utrecht on June 14, 2018

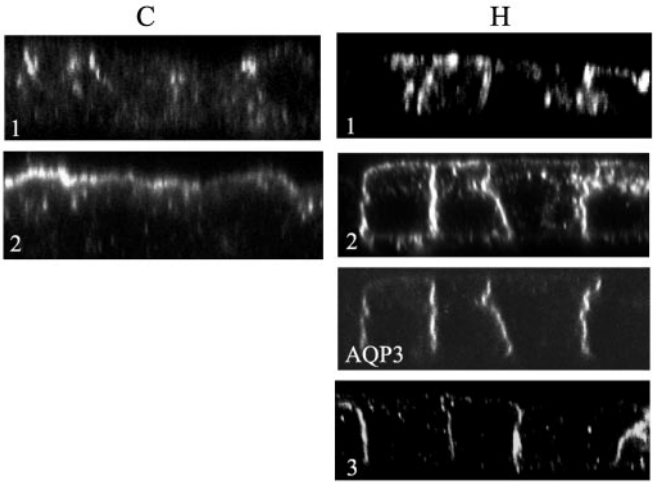

FIG. 4. **With hypertonicity, forskolin induces the translocation of AQP2 to the basolateral instead of apical membrane of MDCK.** X-Z images of AQP2 or AQP3 in MDCK cells are shown. Both in isotonic (*C1*) and hypertonic (*H1*) conditions, AQP2 resides within the intracellular vesicles in nonstimulated cells, but after acute forskolin stimulation, AQP2 is mainly present in the apical membrane under isotonic culturing conditions (*C2*), and in the apical and basolateral membrane when cultured in hypertonic medium using NaCl (*H2*) or mannitol (*H3*) as osmolytes. In hypertonic conditions, AQP2 (*H2*) colocalizes with AQP3 (indicated) in the basolateral membrane.

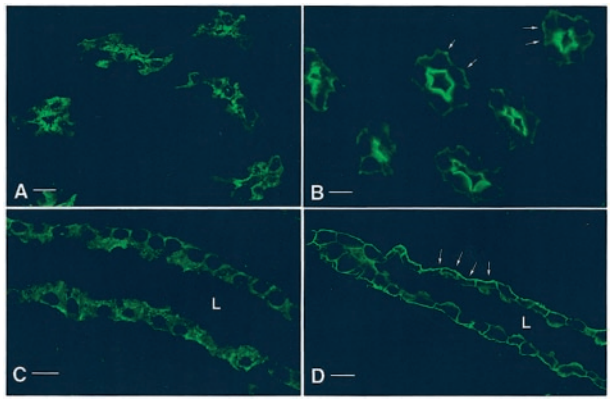

FIG. 5. **Localization of AQP2 in tissue slices from normal rat kidney.** *Panel A* shows AQP2 immunostaining in the proximal inner medulla from a kidney slice that was incubated in buffer alone (for 15 min) to washout endogenous vasopressin. Internalized AQP2 is distributed throughout the cytoplasm of principal cells, although the vesicles tend to be more concentrated toward the apical pole of the cells. After acute (15 min) treatment with vasopressin/forskolin, a bright apical membrane staining and a weaker basolateral membrane staining is detectable in principal cells from the proximal inner medulla (*panel B*). In *panel C*, a collecting duct from the distal inner medulla is shown after 15 min incubation in buffer alone. AQP2 is distributed throughout the cytoplasm of principal cells. After stimulation with vasopressin/forskolin for 15 min, a more than 2-fold increase in basolateral *versus* apical membrane staining is seen in collecting ducts from the distal inner medulla (*panel D,* arrows), compared with that in more proximal regions of the collecting duct (*panel B*). *L*, lumen of the collecting duct. *Bar* = 10 μm.

apical staining was induced after 15 min treatment in the initial portion of the inner medulla, although basolateral staining was also detectable ($_{B/A}$sorting index of 0.39 ± 0.01; n = 15). In more distal regions of the collecting duct, however, the basolateral over apical staining was more than 2-fold higher than in the initial portion (0.87 ± 0.08; n = 15; $p < 0.001$; Fig. 5*D*). In the inner stripe of the outer medulla, AQP2 staining was predominantly apical after AVP/forskolin treatment (not shown), as we have previously described (26). These data support the hypothesis that hypertonicity could be involved in

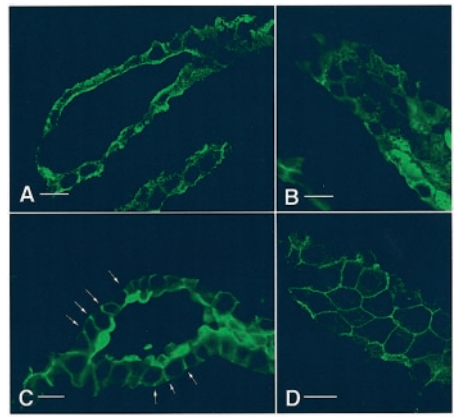

FIG. 6. **Effect of chronic pretreatment with dDAVP on polarity of AQP2 insertion in tissue slices from Brattleboro rats.** *Panel A* shows AQP2 localization in principal cells from the distal inner medullary collecting duct of a control Brattleboro rat, after incubation of kidney slices *in vitro* with vasopressin/forskolin. Staining of the apical pole of the epithelial cells is evident, and some granular staining is also located in the basal region of some cells. *Panel B* shows an oblique section through an inner medullary collecting duct from the same slice to illustrate the low level of basolateral membrane staining under these conditions. *Panels C* and *D* show similar sections through collecting ducts from the distal inner medulla of Brattleboro rats that were pretreated for 11 days with dDAVP prior to the *in vitro* studies. After vasopressin/forskolin treatment of tissues from these rats, a marked basolateral plasma membrane staining was observed (*arrows*), in addition to the apical membrane staining that was evident in some cells (*panel C*). The basolateral, honeycomb pattern is especially evident in the obliquely sectioned collecting duct shown in *Panel D*. This strong basolateral insertion of AQP2 is virtually undetectable in Brattleboro rats that were not pretreated with vasopressin (*panel B*). *Bar* = 10 μm.

determining the polarity of AQP2 distribution, because the most intense basolateral staining was seen in the region of the inner medulla in which interstitial osmolarity is the highest.

Effect of Acute AVP Stimulation on AQP2 Distribution in Kidney Slices from Brattleboro Rats—To test this hypothesis further, we used vasopressin-deficient homozygous Brattleboro rats, which are unable to concentrate their urine, and in which the interstitial osmolarity is reduced compared with normal rats (42). The acute AQP2 insertion response to AVP/forskolin was compared in tissue slices from control, diuretic Brattleboro rats and from Brattleboro rats whose concentration defect had been "corrected" by administration of dDAVP by osmotic minipump for 11 days. As shown in Fig. 6*A*, AQP2 was located at the apical plasma membrane of principal cells from the inner medulla of diuretic Brattleboro rats, although a granular staining was also detected in the basolateral pole of some cells. After acute stimulation of tissue slices from the group of rats chronically treated with dDAVP prior to the *in vitro* experiment, a different AQP2 staining pattern was found. In addition to some apical staining, a very marked basolateral staining was induced, with the staining being especially pronounced along the lateral aspects of principal cells (Fig. 6*C*). This lateral staining was especially evident in tangential sections of tubules in which a bright honeycomb staining pattern, indicative of basolateral AQP2 insertion, was seen in the dDAVP-treated rats (Fig. 6*D*), but not the untreated rats (Fig. 6*B*). These data also indicate that the differential polarized insertion of AQP2 between the two groups resulted from an effect of chronic dDAVP treatment, and did not result from an acute effect of osmolarity, because the osmolarity of the buffer in which the slices were incubated was the same (isotonic) for all experimental groups.

DISCUSSION

Basolateral Localization of AQP2 in MDCK Cells—The present study was designed to investigate potential factors or mech-

Downloaded from http://www.jbc.org/ at Universiteitsbibliotheek Utrecht on June 14, 2018

anisms that might be involved in determining basolateral AQP2 localization. We clearly showed that, besides AQP2 and AQP4, AQP3 is also expressed as a homotetramer. However, while co-expressed in the same cells, AQP2, AQP3, and AQP4 appeared not to co-precipitate, even when overexpressed in *Xenopus* oocytes. Also, immunoprecipitation of AQP2 from Wt10 cells treated with hypertonic medium, a condition that AQP2 and AQP3 co-localize and at which endogenous AQP3 expression is induced, did not result in co-precipitation of AQP3 (not shown). No AQP4 expression was detected in Wt10 cells treated with hypertonic medium. Although we cannot rule out the possibility that in contrast to AQP2–4 homotetramers, AQP2/3 or AQP2/4 heterotetramers disintegrate in 4% desoxycholate, our data strongly indicate that the basolateral routing of AQP2 in principal cells is probably not because of the formation of heterotetramers of AQP2 with basolaterally targeted AQP3 or AQP4. In addition, analysis of MDCK cells expressing high levels of AQP2 driven by the cytomegalovirus promoter did not reveal any detectable staining of the basolateral membrane, which indicates that overexpression of AQP2 is also not a likely cause for its basolateral targeting. This finding is consistent with the fact that basolateral AQP2 expression in the kidney is segment-specific, and is not readily seen in the outer medulla, despite an increase in AQP2 expression levels in all collecting duct segments during dehydration or chronic vasopressin treatment.

Hypertonicity, however, appeared to alter the trafficking of AQP2 in epithelial cells, because AQP2-expressing MDCK cells grown in hypertonic medium for nearly 3 days showed a 14–18 times increase in basolateral over apical membrane insertion of AQP2 after acute forskolin stimulation compared with control cells grown in isotonic medium. In fact, this change in ratio is even underestimated, because to obtain a detectable apical membrane signal for AQP2 in hypertonic Wt10 cells, the AQP2 signal in the basolateral membrane was often saturated. In contrast to AQP2, the distribution of the basolateral protein AQP3 was not altered by growth in hypertonic media.

Basolateral Localization of AQP2 in the Kidney—The role of hypertonicity in AQP2 trafficking was also evaluated using an established *in vitro* kidney slice model in which AVP-induced AQP2 membrane insertion has been previously demonstrated (25, 26). In kidney slices from normally hydrated Sprague-Dawley rats, treatment with a AVP/forskolin mixture resulted a more than 2-fold increase of the AQP2 $_{B/A}$sorting index of principal cells of the distal inner medulla compared with the proximal inner medulla of the same tissue slice. The first segment is the kidney region, which, *in vivo*, is exposed to the highest interstitial osmolarity (up to 1200 mosmol/kg). We have previously shown that in the outer medulla, regulated AQP2 insertion is almost exclusively apical (26). Thus, the polarity of acute insertion of AQP2 in medullary collecting ducts is segment specific, and can be correlated with the level of hypertonicity to which the tubule segments had been exposed *in vivo*.

The data from dDAVP-treated and nontreated Brattleboro rats support this contention. When tissue slices from control, vasopressin-deficient Brattleboro rats were challenged *in vitro* with an AVP/forskolin mixture, apical insertion was seen, although some staining remained at the basolateral pole of the cells. This situation resembled that found in the proximal inner medulla of normal rats. However, the striking basolateral AQP2 insertion detected in the distal inner medulla of slices from Brattleboro rats after chronic pretreatment with dDAVP supports the idea that a high interstitial osmolarity is necessary for this process to occur. Because only tubules from the distal inner medulla showed this marked basolateral staining, a direct effect of dDAVP on this process is unlikely, because principal cells in all kidney regions were exposed to circulating dDAVP.

In addition, even after ~45 min of bathing in an isotonic incubation medium, the *in vivo* environment modulates the subsequent response of collecting ducts in excised tissue slices. This clearly indicated that the effect is not a direct and rapid effect of exposure of cells to an increased osmolarity, but probably reflects a longer term adaptation of the cell to the high interstitial osmolarity that occurs *in vivo* (or nearly 3 days adaptation of MDCK cells to hypertonicity *in vitro*).

Cellular Changes with Hypertonicity—In the short term, a hypertonicity induced cell volume decrease is followed by a regulated volume increase, which is achieved by an influx of inorganic solutes. Over the long term, cells adapt to increased extracellular osmolarity by an intracellular accumulation of organic osmolytes, such as *myo*-inositol, glycerophosphorylcholine, taurine, betaine, and sorbitol (43–45), which is brought about by an increased expression of their transporters. This slow process of adaptation protects the cells from growth retardation and apoptosis, which has been reported to occur with acute high salt challenge in inner medullary collecting duct cells (46). Indeed, acute treatment of our MDCK cells with 375 mosmol of extra NaCl resulted in a significant loss of cells, which precluded the analysis of the short term effect of a hyperosmotic/tonic agent on the localization of AQP2. In addition to the accumulation of inorganic or organic solutes, the process of adaptation to hypertonicity also affects basic cellular functions, such as alterations in cell metabolism, cell growth and differentiation, transcriptional activation, or repression of specific genes and reorganization of cellular structure (via the cytoskeleton; Ref. 47).

These different forms of adaptation to a hypertonic environment are likely to play a role in the redistribution of AQP2 from the apical to the basolateral membrane. In Wt10 cells, the basolateral translocation was observed with membrane-impermeant solutes (NaCl, sucrose, and raffinose), which indicated that hypertonicity (osmotic gradient) and not simply hyperosmolarity (increased solute content) induced the effect. The requirement for hypertonic, rather than hyperosmolar, conditioning provides some insight into upstream events, as it suggests that perturbation of the cell membrane or cytoskeleton may be necessary for AQP2 translocation to occur. Indeed, several studies have reported that osmomechanical stress can activate numerous membrane-associated events including activation of plasma membrane ion channels, calcium signaling events, and phosphatidylinositol turnover (48), which are known to play critical roles in membrane trafficking and cytoskeleton reorganization (49). Of particular relevance to our present observations is that in renal proximal tubule cells, hypoosmotic stress induces exocytosis followed by endocytosis of vesicles at the basolateral membrane and a basolateral-to-apical translocation of vesicles and ion channels (48). Possibly, hyperosmotic stress has the opposite effect of inducing an apical to basolateral translocation of vesicles and associated membrane proteins.

Physiological Relevance of Basolateral AQP2 in the Renal Medulla—In mammals, only cells of the renal medulla are subject to substantial fluctuations in extracellular solute concentrations, because in antidiuresis, medullary cells are confronted with high extracellular NaCl and urea concentrations, which then fall rapidly during the onset of water loading (50). Our present model does not, therefore, explain the basolateral localization of AQP2 in connecting tubules, which are not exposed to significant hypertonicity.

Whereas other factors may be involved in the targeting proc-

Downloaded from http://www.jbc.org/ at Universiteitsbibliotheek Utrecht on June 14, 2018

ess, our study suggests that an increased hypertonicity of the renal medulla might be fundamental to the pronounced basolateral localization of AQP2 in principal cells in antidiuresis. The physiological relevance of this redistribution remains unclear, but three scenarios are possible. First, basolateral AQP2 insertion might be required to increase the water permeability of the basolateral membrane under high flow conditions, despite the presence of AQP3 and AQP4. Second, diversion of AQP2 to the basolateral membrane may be a protective mechanism to limit the apical flow of water and to prevent hypervolemia during prolonged antidiuresis and/or hypernatremia. Third, basolateral AQP2 insertion may represent a transient part of an indirect trafficking pathway in which AQP2 is first delivered basolaterally, followed by internalization and rerouting to the apical membrane by transcytosis. Such an indirect pathway of apical membrane protein insertion has been described for several membrane proteins in other cell types (51).

It is now clear that the same protein, including AQP2, can be inserted into different membrane domains when expressed in different cell types, implying that targeting signals on proteins are not interpreted identically by the sorting machineries of all cells (20, 52–54). However, it is unusual for the polarity of any given protein to be modified under normal physiological, nonpathological conditions. The kidney is largely responsible for maintaining body fluid, electrolyte and acid/base homeostasis, and the remarkable plasticity of epithelial cells in some kidney regions may reflect a continual need to monitor prevailing physiological conditions, and adapt to them by modulating vectorial transport processes across the epithelium. In this organ, systemic acid-base alterations can lead to altered polarity of the H^+-ATPase in collecting duct intercalated cells (55, 56), and we now report that hypertonicity can modify the polarity of AQP2 insertion in principal cells of some regions of the collecting duct. Thus, hypertonicity represents a novel regulatory factor involved in modifying the polarity of membrane protein insertion in the kidney, and possibly in other cell types that are exposed to alterations in their extracellular osmotic environment. Whereas these findings might explain the basolateral localization of AQP2 in the inner medullary collecting duct cells of the kidney, factors involved in basolateral AQP2 expression in the cortex, as well as the physiological/cell biological role of basolateral AQP2 insertion remain to be determined.

Acknowledgment—We thank Dr. W. J. H. Koopman, Department of Cell Physiology, UMC St. Radboud, Nijmegen, for help with setting up the image quantification analysis.

REFERENCES

1. Chou, C. L., Yip, K. P., Michea, L., Kador, K., Ferraris, J. D., Wade, J. B., and Knepper, M. A. (2000) *J. Biol. Chem.* **275,** 36839–36846
2. Brown, D., and Nielsen, S. (2000) in *The Kidney* (Brenner, B., ed) Saunders Co., Orlando, FL
3. Deen, P. M. T., and Brown, D. (2001) in *Trafficking of Native and Mutant Mammalian MIP Proteins* (Hohmann, S., Agre, P., and Nielsen, S., eds) Academic Press, San Diego
4. Deen, P. M. T., and van Os, C. H. (1998) *Curr. Opin. Cell Biol.* **10,** 435–442
5. Nielsen, S., Frokiaer, J., Marples, D., Kwon, T. H., Agre, P., and Knepper, M. A. (2002) *Physiol. Rev.* **82,** 205–244
6. van Os, C. H., Deen, P. M. T., and Dempster, J. A. (1994) *Biochim. Biophys. Acta* **1197,** 291–309
7. Matsumura, Y., Uchida, S., Rai, T., Sasaki, S., and Marumo, F. (1997) *J. Am. Soc. Nephrol.* **8,** 861–867
8. Hozawa, S., Holtzman, E. J., and Ausiello, D. A. (1996) *Am. J. Physiol.* **39,** C1695–C1702
9. Ishibashi, K., Sasaki, S., Fushimi, K., Yamamoto, T., Kuwahara, M., and Marumo, F. (1997) *Am. J. Physiol.* **41,** F235–F241
10. Terris, J., Ecelbarger, C. A., Marples, D., Knepper, M. A., and Nielsen, S. (1995) *Am. J. Physiol.* **38,** F775–F785
11. Nielsen, S., Digiovanni, S. R., Christensen, E. I., Knepper, M. A., and Harris, H. W. (1993) *Proc. Natl. Acad. Sci. U. S. A.* **90,** 11663–11667
12. Deen, P. M. T., Verdijk, M. A. J., Knoers, N. V. A. M., Wieringa, B., Monnens, L. A. H., van Os, C. H., and van Oost, B. A. (1994) *Science* **264,** 92–95
13. Brewer, C. B., and Roth, M. G. (1991) *J. Cell Biol.* **114,** 413–421
14. Lu, M., Lee, M. D., Smith, B. L., Jung, J. S., Agre, P., Verdijk, M. A. J., Merkx, G., Rijss, J. P. L., and Deen, P. M. T. (1996) *Proc. Natl. Acad. Sci. U. S. A.* **93,** 10908–10912
15. Echevarria, M., Windhager, E. E., Tate, S. S., and Frindt, G. (1994) *Proc. Natl. Acad. Sci. U. S. A.* **91,** 10997–11001
16. Kamsteeg, E. J., Wormhoudt, T. A., Rijss, J. P. L., van Os, C. H., and Deen, P. M. T. (1999) *EMBO J.* **18,** 2394–2400
17. Deen, P. M. T., Croes, H., van Aubel, R. A., Ginsel, L. A., and van Os, C. H. (1995) *J. Clin. Invest.* **95,** 2291–2296
18. Richardson, J. C., Scalera, V., and Simmons, N. L. (1981) *Biochim. Biophys. Acta* **673,** 26–36
19. Deen, P. M. T., Rijss, J. P. L., Mulders, S. M., Errington, R. J., van Baal, J., and van Os, C. H. (1997) *J. Am. Soc. Nephrol.* **8,** 1493–1501
20. Deen, P. M. T., van Balkom, B. W., Savelkoul, P. J., Kamsteeg, E. J., Van Raak, M., Jennings, M. L., Muth, T. R., Rajendran, V., and Caplan, M. J. (2002) *Am. J. Physiol.* **282,** F330–F340
21. Mulders, S. M., Bichet, D. G., Rijss, J. P. L., Kamsteeg, E. J., Arthus, M. F., Lonergan, M., Fujiwara, M., Morgan, K., Leijendekker, R., van der Sluijs, P., van Os, C. H., and Deen, P. M. T. (1998) *J. Clin. Invest.* **102,** 57–66
22. Deen, P. M. T., Nielsen, S., Bindels, R. J. M., and van Os, C. H. (1997) *Pflugers Arch.* **433,** 780–787
23. Shayakul, C., Smith, C. P., Mackenzie, H. S., Lee, W. S., Brown, D., and Hediger, M. A. (2000) *Am. J. Physiol.* **278,** F620–F627
24. Gellai, M., Silverstein, J. H., Hwang, J. C., LaRochelle, F. T., Jr., and Valtin, H. (1984) *Am. J. Physiol.* **246,** F819–F827
25. Breton, S., and Brown, D. (1998) *J. Am. Soc. Nephrol.* **9,** 155–166
26. Bouley, R., Breton, S., Sun, T., McLaughlin, M., Nsumu, N. N., Lin, H. Y., Ausiello, D. A., and Brown, D. (2000) *J. Clin. Invest.* **106,** 1115–1126
27. Brown, D., Lydon, J., McLaughlin, M., Stuart-Tilley, A., Tyszkowski, R., and Alper, S. (1996) *Histochem. Cell Biol.* **105,** 261–267
28. Gustafson, C. E., Levine, S., Katsura, T., McLaughlin, M., Aleixo, M. D., Tamarappoo, B. K., Verkman, A. S., and Brown, D. (1998) *Histochem. Cell Biol.* **110,** 377–386
29. Krapivinsky, G., Gordon, E. A., Wickman, K., Velimirovic, B., Krapivinsky, L., and Clapham, D. E. (1995) *Nature* **374,** 135–141
30. Bouvier, M. (2001) *Nat. Rev. Neurosci.* **2,** 274–286
31. Ng, G. Y., Clark, J., Coulombe, N., Ethier, N., Hebert, T. E., Sullivan, R., Kargman, S., Chateauneuf, A., Tsukamoto, N., McDonald, T., Whiting, P., Mezey, E., Johnson, M. P., Liu, Q., Kolakowski, L. F., Jr., Evans, J. F., Bonner, T. I., and O'Neill, G. P. (1999) *J. Biol. Chem.* **274,** 7607–7610
32. Shi, S., Hayashi, Y., Esteban, J. A., and Malinow, R. (2001) *Cell* **105,** 331–343
33. Jordan, B. A., and Devi, L. A. (1999) *Nature* **399,** 697–700
34. Marr, N., Bichet, D. G., Lonergan, M., Arthus, M. F., Jeck, N., Seyberth, H. W., Rosenthal, W., van Os, C. H., Oksche, A., and Deen, P. M. T. (2002) *Hum. Mol. Genet.* **11,** 779–789
35. Hasler, L., Walz, T., Tittmann, P., Gross, H., Kistler, J., and Engel, A. (1998) *J. Mol. Biol.* **279,** 855–864
36. Walz, T., Hirai, T., Murata, K., Heymann, J. B., Mitsuoka, K., Fujiyoshi, Y., Smith, B. L., Agre, P., and Engel, A. (1997) *Nature* **387,** 624–627
37. Neely, J. D., Christensen, B. M., Nielsen, S., and Agre, P. (1999) *Biochemistry* **38,** 11156–11163
38. Jung, J. S., Bhat, R. V., Preston, G. M., Guggino, W. B., Baraban, J. M., and Agre, P. (1994) *Proc. Natl. Acad. Sci. U. S. A.* **91,** 13052–13056
39. Flamion, B., Spring, K. R., and Abramow, M. (1995) *Am. J. Physiol.* **268,** F53–F63
40. Matsuzaki, T., Suzuki, T., and Takata, K. (2001) *Am. J. Physiol.* **281,** C55–C63
41. Ecelbarger, C. A., Terris, J., Frindt, G., Echevarria, M., Marples, D., Nielsen, S., and Knepper, M. A. (1995) *Am. J. Physiol.* **38,** F663–F672
42. Bondy, C. A., Lightman, S. L., and Lightman, S. L. (1989) *Mol. Endocrinol.* **3,** 1409–1416
43. Kwon, H. M., and Handler, J. S. (1995) *Curr. Opin. Cell Biol.* **7,** 465–471
44. Yancey, P. H., Clark, M. E., Hand, S. C., Bowlus, R. D., and Somero, G. N. (1982) *Science* **217,** 1214–1222
45. Sarkadi, B., and Parker, J. C. (1991) *Biochim. Biophys. Acta* **1071,** 407–427
46. Michea, L., Ferguson, D. R., Peters, E. M., Andrews, P. M., Kirby, M. R., and Burg, M. B. (2000) *Am. J. Physiol.* **278,** F209–F218
47. Lang, F., Busch, G. L., Ritter, M., Volkl, H., Waldegger, S., Gulbins, E., and Haussinger, D. (1998) *Physiol. Rev.* **78,** 247–306
48. Reid, J. M., and O'Neil, R. G. (2000) *Biochem. Biophys. Res. Commun.* **271,** 429–434
49. Dove, S. K., McEwen, R. K., Cooke, F. T., Parker, P. J., and Michell, R. H. (1999) *Biochem. Soc. Trans.* **27,** 674–677
50. Beck, F. X., Burger-Kentischer, A., and Muller, E. (1998) *Pflugers Arch.* **436,** 814–827
51. Brown, D., and Stow, J. L. (1996) *Physiol. Rev.* **76,** 245–297
52. Roush, D. L., Gottardi, C. J., Naim, H. Y., Roth, M. G., and Caplan, M. J. (1998) *J. Biol. Chem.* **273,** 26862–26869
53. Pathak, R. K., Yokode, M., Hammer, R. E., Hofmann, S. L., Brown, M. S., Goldstein, J. L., and Anderson, R. G. (1990) *J. Cell Biol.* **111,** 347–359
54. Katsura, T., Verbavatz, J. M., Farinas, J., Ma, T., Ausiello, D. A., Verkman, A. S., and Brown, D. (1995) *Proc. Natl. Acad. Sci. U. S. A.* **92,** 7212–7216
55. Sabolic, I., Brown, D., Gluck, S. L., and Alper, S. L. (1997) *Kidney Int.* **51,** 125–137
56. Bastani, B., Purcell, H., Hemken, P., Trigg, D., and Gluck, S. (1991) *J. Clin. Invest.* **88,** 126–136

Downloaded from http://www.jbc.org/ at Universiteitsbibliotheek Utrecht on June 14, 2018

Hypertonicity Is Involved in Redirecting the Aquaporin-2 Water Channel into the Basolateral, Instead of the Apical, Plasma Membrane of Renal Epithelial Cells

Bas W. M. van Balkom, Marcel van Raak, Sylvie Breton, Nuria Pastor-Soler, Richard Bouley, Peter van der Sluijs, Dennis Brown and Peter M. T. Deen

J. Biol. Chem. 2003, 278:1101-1107.
doi: 10.1074/jbc.M207339200 originally published online October 8, 2002

Access the most updated version of this article at doi: 10.1074/jbc.M207339200

Alerts:
- When this article is cited
- When a correction for this article is posted

Click here to choose from all of JBC's e-mail alerts

This article cites 54 references, 17 of which can be accessed free at
http://www.jbc.org/content/278/2/1101.full.html#ref-list-1

Downloaded from http://www.jbc.org/ at Universiteitsbibliotheek Utrecht on June 14, 2018